Parameter Estimation for Hot-spot Thermal Model of Power Transformers Using Unscented Kalman Filters

Miguel Ángel González-Cagigal, José Antonio Rosendo-Macías, and Antonio Gómez-Expósito, *Fellow, IEEE*

***Abstract*—This paper presents a parameter estimation technique for the hot-spot thermal model of power transformers. The proposed technique is based on the unscented formulation of the Kalman filter, jointly considering the state variables and parameters of the dynamic thermal model. A two-stage estimation technique that takes advantage of different loading conditions is developed, in order to increase the number of parameters which can be identified. Simulation results are presented, which show that the observable parameters are estimated with an error of less than 3%. The parameter estimation procedure is mainly intended for factory testing, allowing the manufacturer to enhance the thermal model of power transformers and, therefore, its customers to increase the lifetime of these assets. The proposed technique could be additionally considered in field applications if the necessary temperature measurements are available.**

***Index Terms*—Parameter estimation, power transformer, unscented Kalman filter, thermal model.**

I. Introduction

INCREASING the life span of costly assets is an essential aspect in the operation and maintenance of power systems. In this regard, the heating of power transformers due to power losses is of paramount importance, which explains the carefully designed cooling systems they have built in, usually based on heat-carrier fluids such as oil.

In order to anticipate the thermal behavior of an oil-immersed power transformer for given load conditions, dynamic thermal models must be somehow considered. This is the case of [1], where a hybrid numerical-analytical technique is proposed, or the bushing thermal model presented in [2] to calculate the hot-spot temperature.

Manuscript received: July 26, 2022; revised: September 7, 2022; accepted: October 12, 2022. Date of CrossCheck: October 12, 2022. Date of online publication: October 26, 2022.

This work was supported by the project HySGrid+ (No. CER-20191019), the project IDENTICAL (No. TP-20210270), and the project FlexOnGrid (No. PID2021-124571OB-I00).

M. Á. González-Cagigal (corresponding author), J. A. Rosendo-Macías, and A. Gómez-Expósito are with the Department of Electrical Engineering, University of Seville, Seville, Spain, and A. Gómez-Expósito is also with ENGREEN Laboratory of Engineering for Energy and Environmental Sustainability, Seville, Spain (e-mail: mgcagigal@us.es; rosendo@us.es; age@us.es).

DOI: 10.35833/MPCE.2022.000439

Finite-element methods (FEMs) can also be used for transformer thermal modeling. Reference [3] includes a 3D magneto-thermal model for the metallic cover (tank) of the transformer, while [4] studies the effect of harmonic conditions in the hot-spot temperature.

Those dynamic thermal models are represented by a system of differential-algebraic equations, involving a set of parameters related to the particular characteristics of the transformer under consideration. An accurate knowledge of these parameters is required to properly calculate the temperature at different points of the transformer. In this context, parameter estimation techniques can be applied to the dynamic thermal model of the power transformer, such as those used in [5], where the sensitivity of the estimated parameters in linear and nonlinear regression models is analyzed. Genetic algorithms are also considered for this purpose in [6].

In this paper, a dynamic state estimator (DSE) based on Kalman filter (KF) is used for the joint estimation of state variables and parameters arising in the hot-spot thermal model of power transformers, as defined in the IEC 60076-7-2018 [7]. The KF-based DSE has been used in a remarkable number of studies for state estimation in power systems [8], [9]. Regarding parameter estimation, two types of implementations can be distinguished, namely: a joint state and parameter estimation [10]-[12], and a dual estimation where two different estimators are sequentially applied at each time instant [13]. A particular formulation of the KF for nonlinear systems, the so-called unscented KF (UKF), is considered in this paper for a joint estimation of the state and parameters. This estimation technique has been widely used in the studies related to electric power systems [14]-[16], and its results have been proven accurate when applied to strongly nonlinear systems such as the fully-regulated synchronous generator [17].

A preliminary academic work [18] has concluded that it is impossible to estimate the whole set of parameters arising in the hot-spot thermal model solely from oil temperature measurements. To overcome this issue, this paper proposes a two-stage estimation technique, which considers measurements of the hot-spot temperature taken under different loading conditions, increasing in this way the number of observable parameters.

The remainder of this paper is organized as follows. Sec-

tion II reviews the UKF algorithm. Section III presents the modeling of hot-spot dynamic thermal model of power transformers. The implementation of the UKF is described in Section IV. Section V presents a case study to test the accuracy of the proposed technique, including a comparison with an alternative non-linear KF implementation. Finally, the conclusions are presented in Section VI.

II. UKF Algorithm

KF implementations require a set of state equations, including the dynamic and the measurement equations. In the case of continuous-time, discrete-measurement non-linear systems, these equations can be expressed as:

$$\dot{\boldsymbol{x}}(t)=\boldsymbol{f}(\boldsymbol{x}(t),\boldsymbol{u}(t))+\boldsymbol{w}(t) \tag{1}$$

$$\boldsymbol{z}(t_k)=\boldsymbol{g}(\boldsymbol{x}(t_k),\boldsymbol{u}(t_k))+\boldsymbol{v}(t_k) \tag{2}$$

where $\boldsymbol{x}(t)$ is the state vector; $\boldsymbol{f}(\cdot)$ is the state function; $\boldsymbol{g}(\cdot)$ is the measurement function; $\boldsymbol{u}(t)$ is the system input; $\boldsymbol{z}(t_k)$ is the measurement vector at instant t_k; and $\boldsymbol{w}(t)$ and $\boldsymbol{v}(t_k)$ are the model and measurement noises, which are assumed Gaussian processes with covariance matrices $\boldsymbol{Q}$ and $\boldsymbol{R}$, respectively.

Considering a time step Δt, the above equations have the following discrete counterparts:

$$\boldsymbol{x}_k=\boldsymbol{x}_{k-1}+\boldsymbol{f}(\boldsymbol{x}_{k-1},\boldsymbol{u}_{k-1})\Delta t+\boldsymbol{w}_k \tag{3}$$

$$\boldsymbol{z}_k=\boldsymbol{g}(\boldsymbol{x}_k,\boldsymbol{u}_k)+\boldsymbol{v}_k \tag{4}$$

Equations (3) and (4) are more appropriate for non-linear Kalman filtering techniques such as extended KF (EKF), which simply linearizes the state function $\boldsymbol{f}(\boldsymbol{x}(t),\boldsymbol{u}(t))$ in (3), and the UKF.

Previous experiences on the application of the EKF to the equations that describe the dynamic behavior of synchronous machines, and their regulators, have not provided satisfactory results [17]. Therefore, this paper makes use of the UKF, whose implementation is based on an iterative process with two different stages [19].

A. Prediction Stage

At instant k, a cloud of $2L+1$ vectors, called σ-points, is calculated from the previous estimate or expected value of the state vector $\hat{\boldsymbol{x}}_{k-1}$ (dimension L) and the covariance matrix of the state estimation error $\boldsymbol{P}_{k-1}$ using the following expression:

$$\begin{cases}\boldsymbol{x}_{k-1}^{0}=\hat{\boldsymbol{x}}_{k-1}\\ \boldsymbol{x}_{k-1}^{i}=\hat{\boldsymbol{x}}_{k-1}+\left(\sqrt{(L+\lambda)\boldsymbol{P}_{k-1}}\right)_i & i=1,2,...,L\\ \boldsymbol{x}_{k-1}^{i+L}=\hat{\boldsymbol{x}}_{k-1}-\left(\sqrt{(L+\lambda)\boldsymbol{P}_{k-1}}\right)_{i+L} & i=1,2,...,L\end{cases} \tag{5}$$

where $\left(\sqrt{(L+\lambda)\boldsymbol{P}_{k-1}}\right)_i$ is the i^{th} column of the matrix $\sqrt{(L+\lambda)\boldsymbol{P}_{k-1}}$; and λ is a scaling factor calculated from (6) with α and κ being two filter parameters to be tuned.

$$\lambda=\alpha^2(L+\kappa)-L \tag{6}$$

The σ-points are evaluated using (3), yielding $2L+1$ vectors $\boldsymbol{x}_k^{i-}$ from which the a-priori estimations $\hat{\boldsymbol{x}}_k^-$ and $\boldsymbol{P}_k^-$ are obtained as the weighted mean and covariance of those vectors:

$$\hat{\boldsymbol{x}}_k^-=\sum_{i=0}^{2L}W_{mi}\,\boldsymbol{x}_k^{i-} \tag{7}$$

$$\boldsymbol{P}_k^-=\sum_{i=0}^{2L}W_{ci}(\boldsymbol{x}_k^{i-}-\hat{\boldsymbol{x}}_k^-)(\boldsymbol{x}_k^{i-}-\hat{\boldsymbol{x}}_k^-)^{\mathrm{T}}+\boldsymbol{Q}_k \tag{8}$$

where W_{mi} and W_{ci} are the i^{th} elements of weighting vectors $\boldsymbol{W}_m$ and $\boldsymbol{W}_c$, respectively, which are calculated as:

$$\begin{cases}W_{m0}=\dfrac{\lambda}{L+\lambda}\\ W_{c0}=\dfrac{\lambda}{L+\lambda}+1-\alpha^2+\beta\\ W_{mi}=W_{ci}=\dfrac{1}{2(L+\lambda)} & i=1,2,...,2L\end{cases} \tag{9}$$

where β is another tunable parameter; and the values of parameters α, β, and κ considered in this paper will be provided in Section V.

B. Correction Stage

On the basis of the a-priori estimations, a new cloud of vectors is calculated by means of similar expressions to those used in the prediction stage for the σ-points:

$$\begin{cases}\boldsymbol{x}_k^{0-}=\hat{\boldsymbol{x}}_k^-\\ \boldsymbol{x}_k^{i-}=\hat{\boldsymbol{x}}_k^-+\left(\sqrt{(L+\lambda)\boldsymbol{P}_k^-}\right)_i & i=1,2,...,L\\ \boldsymbol{x}_k^{(i+L)-}=\hat{\boldsymbol{x}}_k^--\left(\sqrt{(L+\lambda)\boldsymbol{P}_k^-}\right)_{i+L} & i=1,2,...,L\end{cases} \tag{10}$$

In this case, the vectors are evaluated through the measurement function $\boldsymbol{g}(\boldsymbol{x}_k,\boldsymbol{u}_k)$ in (4), yielding

$$\boldsymbol{\gamma}_k^{i-}=\boldsymbol{g}(\boldsymbol{x}_k^{i-},\boldsymbol{u}_k)\quad i=0,1,...,2L \tag{11}$$

The a-priori measurement estimation $\hat{\boldsymbol{z}}_k^-$ is calculated as the weighted mean of the previous points using the vector $\boldsymbol{W}_m$ defined by (9):

$$\hat{\boldsymbol{z}}_k^-=\sum_{i=0}^{2L}W_{mi}\,\boldsymbol{\gamma}_k^{i-} \tag{12}$$

Then, the covariance matrix of the measurement estimation error $\boldsymbol{P}_{zk}^-$ and the cross-covariance matrix of state and measurements $\boldsymbol{P}_{xzk}^-$ are obtained using vector $\boldsymbol{W}_c$ as:

$$\boldsymbol{P}_{zk}^-=\sum_{i=0}^{2L}W_{ci}(\boldsymbol{\gamma}_k^{i-}-\hat{\boldsymbol{z}}_k^-)(\boldsymbol{\gamma}_k^{i-}-\hat{\boldsymbol{z}}_k^-)^{\mathrm{T}}+\boldsymbol{R}_k \tag{13}$$

$$\boldsymbol{P}_{xzk}^-=\sum_{i=0}^{2L}W_{ci}(\boldsymbol{x}_k^{i-}-\hat{\boldsymbol{x}}_k^-)(\boldsymbol{\gamma}_k^{i-}-\hat{\boldsymbol{z}}_k^-)^{\mathrm{T}} \tag{14}$$

By using the a-priori estimations at instant k from (7) and (8) and the Kalman gain in (15), the respective a-posteriori estimations can be obtained from (16) and (17), both of which are necessary for the next step.

$$\boldsymbol{K}_k=\boldsymbol{P}_{xzk}^-(\boldsymbol{P}_{zk}^-)^{-1} \tag{15}$$

$$\hat{\boldsymbol{x}}_k=\hat{\boldsymbol{x}}_k^-+\boldsymbol{K}_k(\boldsymbol{z}_k-\hat{\boldsymbol{z}}_k^-) \tag{16}$$

$$\boldsymbol{P}_k=\boldsymbol{P}_k^-\boldsymbol{K}_k\boldsymbol{P}_{zk}^-\boldsymbol{K}_k^{\mathrm{T}} \tag{17}$$

C. Parameter Estimation

State estimation requires the previous knowledge of the parameters involved in the dynamic model. However, when these parameters are not known, estimation techniques such as UKF can be used for a joint estimation of state variables and parameters [20]. In this way, an augmented state vector $\boldsymbol{x}_a^{\mathrm{T}}=[\boldsymbol{x}^{\mathrm{T}},\boldsymbol{\psi}^{\mathrm{T}}]$ is adopted, where $\boldsymbol{x}$ contains the state variables and $\boldsymbol{\psi}$ includes the model parameters to be identified. Then, the dynamic model (3) and (4) is replaced by the following augmented equations.

$$\begin{bmatrix}\boldsymbol{x}_k\\ \boldsymbol{\psi}_k\end{bmatrix}=\begin{bmatrix}\boldsymbol{x}_{k-1}+f(\boldsymbol{x}_{k-1},\boldsymbol{\psi}_{k-1},\boldsymbol{u}_{k-1})\Delta t\\ \boldsymbol{\psi}_{k-1}\end{bmatrix}+\boldsymbol{w}_k \tag{18}$$

$$\boldsymbol{z}_k=\boldsymbol{g}(\boldsymbol{x}_{ak},\boldsymbol{u}_k)+\boldsymbol{v}_k \tag{19}$$

where $\boldsymbol{w}_k$ is now the augmented-model noise vector including the state variable components, and the parameter components.

III. Modeling of Hot-spot Dynamic Thermal Model of Power Transformers

As stated above, the evolution of the thermal state of a power transformer can be characterized in many ways, depending on the required accuracy, transformer size, available sensors, and cooling system. For oil-immersed power transformers, the IEC 60076-7-2018 standard [7] considers a simple thermal model, based on a single worst-case temperature (so-called hot-spot temperature), aimed at capturing the impact on transformer life of operation under different ambient temperatures and load conditions. This hot-spot model is deemed sufficiently accurate to characterize the operating temperatures that impact the transformer thermal aging. Therefore, it can be useful to improve the operation and control of this important asset, as well as in the planning stages to define its thermal rating.

In this section, the standard hot-spot model, used as the reference model for simulation purposes, is first described. Then, a more compact simplified model that involves a subset of observable parameters is also presented and discussed. This will be the model actually considered by the KF-based parameter estimator.

A. Full Hot-spot Model

The dynamic equations adopted in the reference model, i. e., the model used in the case study below to simulate noisy measurements, are directly taken from [7].

First, the evolution of the top-oil temperature θ_o is characterized through the following expression:

$$\dot{\theta}_o=\frac{1}{k_{11}\tau_o}\left[\left(\frac{1+K^2R}{1+R}\right)^x\Delta\theta_{or}-(\theta_o-\theta_a)\right] \tag{20}$$

where θ_a is the ambient temperature; K is the transformer load factor, which is defined as the quotient between the current through the transformer and the rated one; $\Delta\theta_{or}$ is the oil temperature rise under rated-load conditions; k_{11} is a constant of the thermal model; τ_o is the oil time constant; x is the total loss exponent; and R is the ratio between rated-load and no-load losses. The hot-spot temperature is related to the top-oil temperature through two intermediate state variables $\Delta\theta_{h1}$ and $\Delta\theta_{h2}$ with different dynamics, which are described as:

$$\Delta\dot{\theta}_{h1}=\frac{1}{k_{22}\tau_w}(k_{21}K^y\Delta\theta_{hr}-\Delta\theta_{h1}) \tag{21}$$

$$\Delta\dot{\theta}_{h2}=\frac{k_{22}}{\tau_o}[(k_{21}-1)K^y\Delta\theta_{hr}-\Delta\theta_{h2}] \tag{22}$$

where k_{21} and k_{22} are the constants of the thermal model; τ_w is the winding time constant; y is the current exponent; and $\Delta\theta_{hr}$ is the hot-spot temperature rise under rated load conditions.

Finally, the hot-spot temperature θ_h can be calculated as:

$$\theta_h=\theta_o+\Delta\theta_{h1}-\Delta\theta_{h2} \tag{23}$$

This hot-spot temperature is located towards the top of the transformer winding, given that the degradation of the solid insulation with high temperatures is typically taken as the main aging factor.

B. Simplified Estimation Model

The whole set of parameters involved in (20)-(22) is not observable when the temperature measurements discussed in Section IV (oil and hot-spot temperatures) are regularly captured during the transformer operation. Therefore, in order to obtain the values of those parameters, more sophisticated methods should be considered, involving specific tests for the thermal properties of the cooling system [21].

In this case, the lack of observability of some model parameters is caused by the unique way in which those parameters appear in the hot-spot model equations, which prevents their values to be estimated separately. In particular, the four parameters k_{11}, k_{22}, τ_o, and τ_w, involved in (20)-(22), appear combined in only three different ways ($k_{11}\tau_0$, $k_{22}\tau_w$, and k_{22}/τ_o), so they cannot be estimated independently.

To overcome the observability problem, the alternative explored in this paper consists of algebraically rearranging the original full model, by introducing a smaller number of equivalent parameters, which leads to a more compact and more linear, yet accurate dynamic model to be handled by the KF-based parameter estimator. The goal is to transform the original nonlinear model (20)-(22) into the following dynamic model:

$$\dot{\theta}_o=\frac{1}{T_o}[A\Delta\theta_{or}-(\theta_o-\theta_a)] \tag{24}$$

$$\Delta\dot{\theta}_{h1}=\frac{1}{T_1}(C_1B-\Delta\theta_{h1}) \tag{25}$$

$$\Delta\dot{\theta}_{h2}=\frac{1}{T_2}(C_2B-\Delta\theta_{h2}) \tag{26}$$

where in addition to the original parameter $\Delta\theta_{or}$, five modified parameters T_o, T_1, T_2, C_1, C_2 and two auxiliary parameters A and B are introduced, which are related to those in the full hot-spot model as follows: $T_o=k_{11}\tau_o$; $T_1=k_{22}\tau_w$; $T_2=\tau_o/k_{22}$; $C_1=k_{21}\Delta\theta_{hr}$; $C_2=(k_{21}-1)\Delta\theta_{hr}$; $A=[(1+K^2R)/(1+R)]^x$; and $B=K^y$.

The following remarks are made:

1) The three time constants T_o, T_1, and T_2 embed four parameters k_{11}, k_{22}, τ_o, and τ_w. So, the compact model, besides

being more linear, gets rid of a parameter without losing any accuracy, as there is no need in practice to determine individually the four parameters embedded in those time constants.

2) The constants C_1 and C_2, once estimated, allow computing the two parameters k_{21} and $\Delta\theta_{hr}$. So, the advantage of using C_1 and C_2 has to do with the enhanced linearity of the resulting model (products are avoided).

3) As can be noticed, the values of the auxiliary parameters A and B depend on the operating point of the power transformer. The technique proposed in this paper estimates the transformed parameters considering different load factors (K) and then letting the transformer reach the steady-state thermal conditions for each value of K. This provides different estimations of A and B, which are in turn used to compute estimates of the original parameters R, x, and y. From the defining expressions of the auxiliary parameters, it can be concluded that at least two estimations of A are required to obtain the original parameters R and x, while a single value of B would suffice to calculate y.

In a nutshell, if the reduced set of parameters involved in the model (24)-(26) can be estimated (including at least two estimations of A), the dynamics of the hot-spot temperature can be fully characterized according to the standard definition, but rather using the alternative set of parameters $\Delta\theta_{or}$, T_o, T_1, T_2, C_1, C_2, R, x, and y, proposed in this paper. Regarding the original parameters involved in the hot-spot model, $\Delta\theta_{or}$ is directly obtained in the estimation process, while k_{21} and $\Delta\theta_{hr}$ can be computed using the estimated values of the modified parameters C_1 and C_2. Finally, as mentioned before, R, x, and y are obtained using estimates of A and B.

IV. Implementation of UKF

Early attempts to implement the KF-based estimation, including the whole set of modified parameters in the model, led to convergence problems. To overcome this issue, a two-stage estimation technique is proposed in this paper.

A. The First Stage: Full-load Conditions

At this stage, the transformer is assumed to serve the rated load ($K=1$), starting from no-load conditions ($K=0$) or any other intermediate value. In this situation, both parameters A and B are equal to 1, regardless the values of x, y, and R. Therefore, (24)-(26) can be rewritten as:

$$\dot{\theta}_o = \frac{1}{T_o}\left[\Delta\theta_{or} - (\theta_o - \theta_a)\right] \tag{27}$$

$$\dot{\Delta\theta}_{h1} = \frac{1}{T_1}\left(C_1 - \Delta\theta_{h1}\right) \tag{28}$$

$$\dot{\Delta\theta}_{h2} = \frac{1}{T_2}\left(C_2 - \Delta\theta_{h2}\right) \tag{29}$$

In this case, the state vector is defined as:

$$\boldsymbol{x}^{\mathrm{T}} = [\theta_o \quad \Delta\theta_{h1} \quad \Delta\theta_{h2}] \tag{30}$$

While the parameter vector $\boldsymbol{\psi}$ reduces to (31), leading to a total vector size $L=9$ (rather than 11).

$$\boldsymbol{\psi}^{\mathrm{T}} = [T_1 \quad T_2 \quad C_1 \quad C_2 \quad \Delta\theta_{or} \quad T_o] \tag{31}$$

Four magnitudes are assumed to be measured or known, namely: K, θ_a, θ_o, and θ_h. In the proposed formulation, these magnitudes are divided into inputs $\boldsymbol{u}=[K, \theta_a]$ and measurements $\boldsymbol{z}=[\theta_o, \theta_h]$ [22]. The input K (load factor) is derived from the current through the transformer, which causes the heating in the oil and windings.

The vector $\boldsymbol{z}$ needs to be formulated in terms of the augmented state and input vectors, as in (19). The first component of $\boldsymbol{z}$, i.e., the oil temperature θ_o, is a trivial case, since it is directly a state variable. For the hot-spot temperature θ_h, (23) is used.

B. The Second Stage: Intermediate Loads

The goal of the second stage is to estimate the parameters A and B. For this purpose, two intermediate loading points, K_1 and K_2, with $K_1 > 0$ and $K_2 < 1$ are enforced, both under steady-state conditions. This provides two different estimations of the synthetic parameters A and B, from which the original parameters R, x, and y can be calculated. Both state transitions can start from $K=0$ or any other intermediate value, as shown in the case study.

In this case, the parameter vector $\boldsymbol{\psi}$ contains only A and B, as the remaining modified parameters can be set to be their values estimated at the first stage. The state vector $\boldsymbol{x}$ is the same as at the first stage, yielding a size $L=5$ for the augmented state vector $\boldsymbol{x}_a$ at the second stage. Similar considerations as at the first stage can be made regarding the measurements used in the UKF implementation.

V. Case Study

In this section, the proposed parameter estimation technique is tested using synthetic measurements obtained from the full hot-spot model presented in Section III, where the model parameters are assumed to be perfectly known. Indeed, it is only in simulation environments that estimation errors can be thoroughly evaluated. Note that the rated power and voltage of the transformer are irrelevant for our purposes, as the transformer load factor K is in per unit and the physical characteristics of the apparatus are reflected in the parameters defining the hot-spot thermal model. In any case, this paper is mainly focused on three-phase distribution transformers.

A. In-house Estimation of Hot-spot Dynamic Model

It is assumed that the manufacturer performs the required factory tests (the two stages described before) on a representative transformer, in order to duly characterize the whole series of transformers of the same rated power and voltage, manufactured with the same materials. Those tests involve oil and hot-spot temperature measurements. For the simulations, the ambient temperature is assumed to evolve as in Fig. 1 [23]. The time step considered in this work is $\Delta t = 1$ min.

The parameter values considered for the simulation are taken from the IEC 60076-7-2018 standard (for distribution transformers up to 2500 kVA of rated power), which are summarized in Table I. However, the proposed technique is suitable for other rated power ranges.

Starting from no-load conditions ($K=0$), the transformer is sequentially subjected to three identical load steps, each equal to 1/3 of the rated load. The load factor profile, along with the evolution of the oil and hot-spot temperatures, is shown in Fig. 2, where 2% error has been artificially added to the measurements. Since the largest time constant in the simulated system is in the order of 3 hours, the simulation time is set to be 9 hours for each load step ($K=1/3$, $K=2/3$, and $K=1$), i.e., three times the time constant, so as to make sure that steady-state conditions are reached for each loading point.

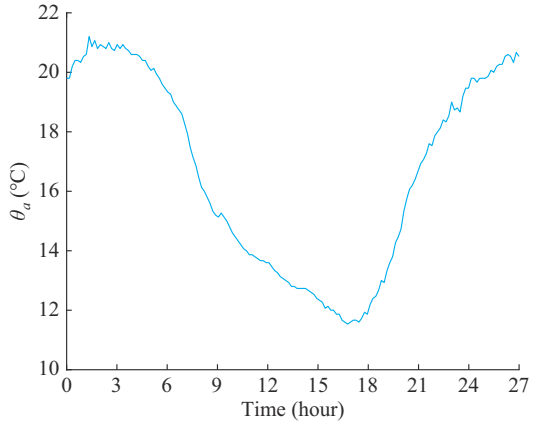

Fig. 1. Considered profile for ambient temperature.

TABLE I
PARAMETER VALUES FOR SIMULATION

Parameter	Simulation value	Parameter	Simulation value
$\Delta\theta_{or}$	55 °C	$\Delta\theta_{hr}$	23 °C
k_{11}	1 p.u.	k_{22}	2 p.u.
τ_o	180 min	k_{21}	1.5 p.u.
R	5 p.u.	τ_w	4 min
x	0.8 p.u.	y	1.6 p.u.

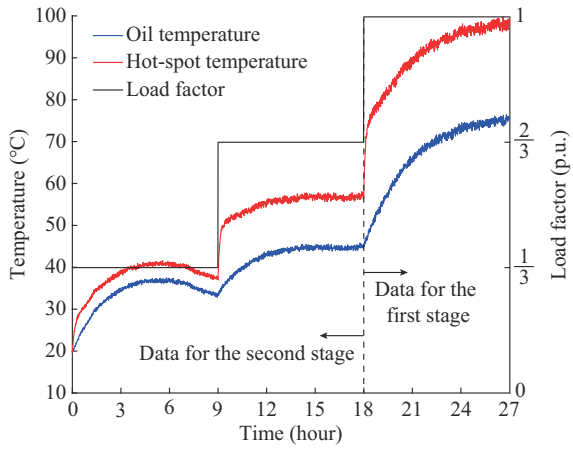

Fig. 2. Evolution of load factor and noisy measurements.

As noted in the figure, the information corresponding to the transition from $K=2/3$ to $K=1$ will be used for the first stage of the proposed technique, while the measurements from the first two load steps will be used for the second stage.

The UKF algorithm has been implemented with $\alpha=10^{-4}$, $\kappa=0$, and $\beta=2$ according to [24], where the influence of these scaling parameters is analyzed, while typical values are considered for the covariance matrices $\boldsymbol{P}_0$, $\boldsymbol{Q}$, and $\boldsymbol{R}$. The values of the modified parameters are initialized randomly, in a range between ±20% and ±40% of their simulated values.

The proposed two-stage estimation technique presents a consistent performance in its ability to properly estimate the modified model parameters. Figure 3 shows the estimation results obtained from the first stage of the proposed technique. The evolution of the estimation error covariance is also included in this figure. For each parameter i, its estimated value is represented along with a three-σ band $\pm 3\sqrt{P_{ii}}$ (gray areas). The resulting relative errors are summarized in Table II, from which it is concluded that the maximum relative error remains under 3%.

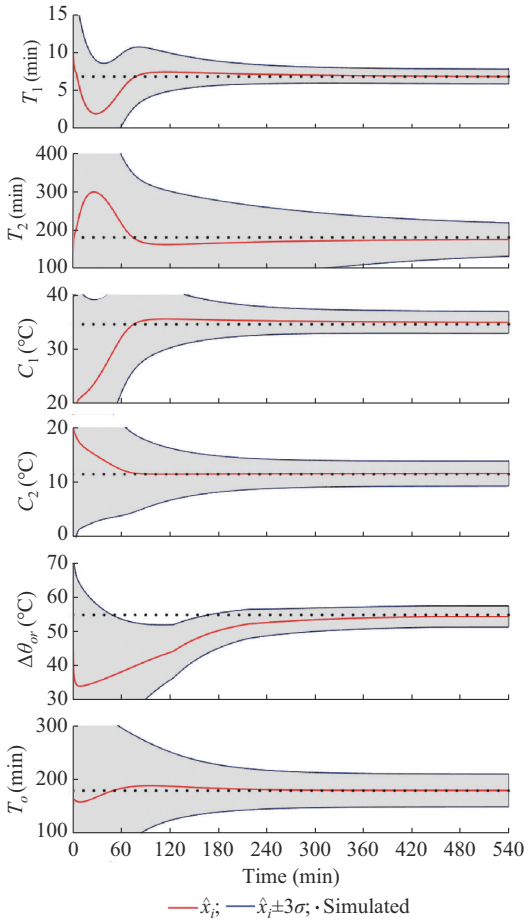

Fig. 3. Estimation results obtained from the first stage of proposed technique.

TABLE II
RELATIVE ERROR IN PARAMETER ESTIMATION AT THE FIRST STAGE

Value	T_1 (min)	T_2 (min)	C_1 (°C)	C_2 (°C)	$\Delta\theta_{or}$ (°C)	T_o (min)
Simulated	8.000	180.000	34.500	11.500	55.000	180.000
Estimated	8.004	174.463	34.873	11.612	54.528	180.432
Relative error (%)	0.046	2.985	1.082	0.977	0.858	0.240

At the second stage, the value of the load is suddenly changed, first from $K=0$ to $K=1/3$ and then, at $t=540$ min, from $K=1/3$ to $K=2/3$. The total simulation time is 1080 min in this case. Only the parameters A and B are included in the vector $\boldsymbol{\psi}$, while the remaining modified parameters are given their values estimated at the first stage. Regarding the KF tuning (initial values for $\hat{\boldsymbol{x}}_{a0}$ and the matrices $\boldsymbol{P}_0$, $\boldsymbol{Q}$, and $\boldsymbol{R}$), the similar assumptions to those at the first stage are made.

The estimation results obtained from the auxiliary parameters A and B at the second stage are shown in Fig. 4, where the deviations $\hat{x}_i \pm 3\sqrt{P_{ii}}$ are also highlighted by the gray areas.

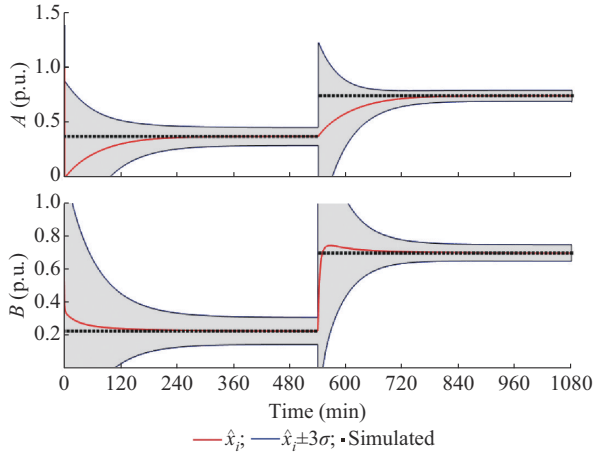

Fig. 4. Estimated results obtained from auxiliary parameters A and B at the second stage.

With the estimated values for $K=1/3$ and $K=2/3$, the original parameters R, x, and y can be calculated using a solver, yielding the estimated values and the relative errors included in Table III. In this paper, a MATLAB function is used for the implementation of the solver.

TABLE III
RELATIVE ERRORS IN PARAMETER ESTIMATION AT THE SECOND STAGE

Value	R (p.u.)	x (p.u.)	y (p.u.)
Simulated	5.000	0.800	1.600
Estimated	4.969	0.802	1.575
Relative error (%)	0.602	0.247	1.562

As previously mentioned, two intermediate loads are theoretically sufficient to estimate the modified parameters A and B at the second stage of the proposed technique. In order to check the sensitivity of the results to the use of redundant (i.e., more than two) load factors, an additional scenario is simulated with four intermediate loads ($K=0.2$, 0.4, 0.6, and 0.8). Then, the resulting estimates of A and B are introduced in a least-squares function from MATLAB, in order to obtain new estimations for the original parameters R, x, and y. As can be observed in Table IV, the resulting relative errors are similar to those presented in Table III for two intermediate loads.

TABLE IV
RELATIVE ERRORS AT THE SECOND STAGE WITH FOUR INTERMEDIATE LOADS

Value	R (p.u.)	x (p.u.)	y (p.u.)
Simulated	5.000	0.800	1.600
Estimated	4.972	0.806	1.579
Relative error (%)	0.560	0.749	1.312

Finally, Table V summarizes the relative errors of the observable original parameters in the hot-spot model which can be obtained from the estimated values of the modified parameters.

TABLE V
RELATIVE ERRORS OF OBSERVABLE ORIGINAL PARAMETERS

Value	$\Delta\theta_{or}$ (°C)	k_{21} (p.u.)	$\Delta\theta_{hr}$ (°C)	R (p.u.)	x (p.u.)	y (p.u.)
Simulated	55.000	1.5000	23.000	5.000	0.800	1.600
Estimated	54.528	1.499	23.261	4.969	0.802	1.575
Relative error (%)	0.858	0.053	1.135	0.602	0.247	0.155

In order to assess the performance of the UKF with increasing measurement noise, Table VI includes the maximum relative error in the parameter estimation for different noise levels. As expected, the estimates deteriorate with higher noise levels, but the maximum relative error still remains under 8% even for an unrealistic 10% measurement error.

TABLE VI
THE MAXIMUM RELATIVE ERROR IN PARAMETER ESTIMATION FOR DIFFERENT NOISE LEVELS

Noise level (%)	The maximum relative error (%)
2	2.985
5	4.021
10	7.533

B. Comparison with EKF Formulation

The results obtained with the UKF formulation are compared in this subsection with those provided by the EKF, which is a popular alternative for non-linear dynamic estimation based on the linearization of the model. Although both KFs adopt the same simplified model presented in Section III, the EKF requires the computation of Jacobian matrices (partial derivatives with respect to the variables in the augmented state vector), as provided in Appendix A.

Similar assumptions are made regarding the test conditions for the case study, with two stages in the estimation process and the same step changes in the load factor K. First, Fig. 5 represents the comparison of the estimated value of C_2. In this figure, it is observed that the EKF presents a remarkably higher estimation error compared with that of the proposed technique using UKF. The reason for this lower accuracy of the EKF formulation relates to the strong nonlinearities arising in the estimation model. Despite the modi-

fied model proposed in this paper being more linear, it involves the product of some parameters in the augmented state vector, making the problem in hand still non-linear. This deteriorates the performance of the EKF (first-order approximation of the covariance) when compared with that of the UKF, which approximates the covariance of the estimation error up to the third order [19].

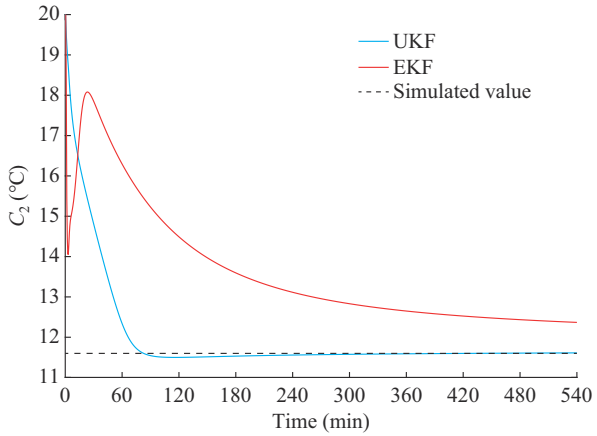

Fig. 5. Comparison of estimated value of C_2.

Table VII compares the relative errors provided by each tested algorithm (UKF and EKF) for the whole set of modified parameters. As can be observed, the estimation errors are unacceptable, particularly regarding parameters T_1, T_2, and C_2.

TABLE VII
COMPARISON OF RELATIVE ERRORS PROVIDED BY UKF AND EKF ALGORITHMS

Parameter	Relative error (%)	
	EKF	UKF
T_1	4.144	0.046
T_2	20.585	2.985
C_1	1.013	1.082
C_2	7.690	0.977
$\Delta\theta_{or}$	0.817	0.858
T_o	1.468	0.240
R	1.014	0.602
x	1.120	0.247
y	0.534	0.155

In light of these results, it can be concluded that the performance of the proposed UKF-based technique is superior to that of the EKF-based technique.

C. Impact of Parameter Estimation Errors on Hot-spot Temperature Estimation

Once the parameters of the thermal model have been estimated with the proposed UKF-based technique, it is important to assess if the estimation errors of the hot-spot temperature are acceptable. For this purpose, two separate simulations have been carried out.

1) Simulation using the exact value of the model parameters, the so-called exact model.

2) Simulation considering the estimated values of the original and modified parameters presented in the previous section (Tables II and III), namely the estimated model.

In both cases, the total simulation time is one week and the system inputs (ambient temperature and load factor) are the same, with a typical evolution for the ambient temperature, as shown in Fig. 1, and a cyclic variation of the transformer load, as shown in Fig. 6 (the daily load profile is based on [7]). Note that, unlike in the factory tests, no oil measurements are captured (only the ambient temperature is used as input).

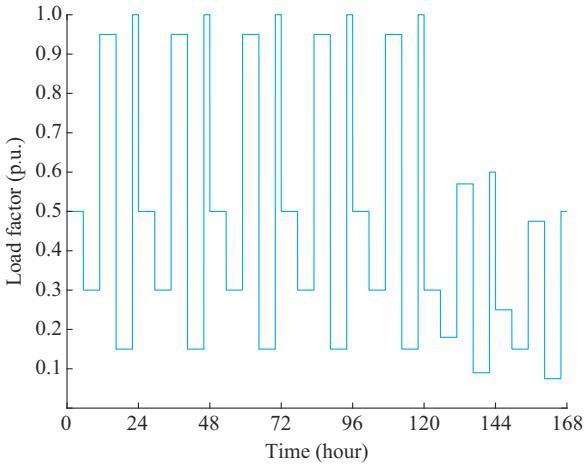

Fig. 6. Load profile for one-week simulation.

The evolution results of the hot-spot temperatures for both models and the corresponding error are represented in Fig. 7. In light of this figure, the following remarks can be made.

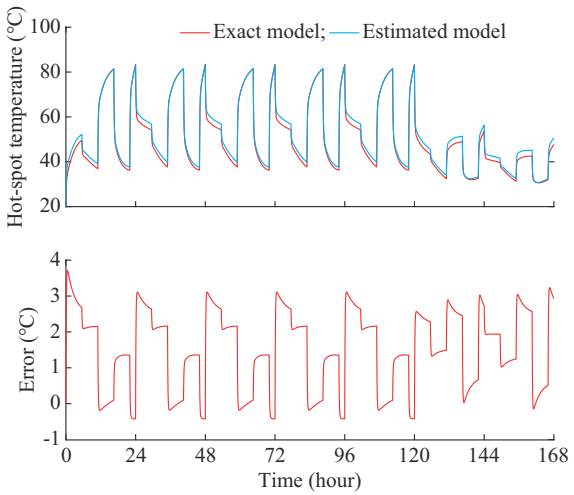

Fig. 7. Evolution results of hot-spot temperatures and corresponding error.

1) The maximum hot-spot temperature error is lower than 4℃, providing evidence of the accuracy of the estimated model.

2) In most cases, the hot-spot temperature obtained with the estimated model is higher than that with the exact model (safe side).

3) Interestingly, lower errors (even negligible) are ob-

tained when the transformer load is high and the hot-spot temperatures reach the highest values. Reciprocally, the periods of higher estimation errors correspond to the reduced values of the hot-spot temperature, when the integrity of the transformer is not jeopardized.

VI. Conclusion

In this paper, an UKF is developed, implemented, and tested to estimate the state variables and parameters of the hot-spot dynamic thermal model of a power transformer. The non-observability of the parameters involved in the original thermal model is circumvented by introducing a reduced but equivalent set of modified parameters.

Additionally, to overcome the convergence problems arising when the whole set of parameters is simultaneously handled, a two-stage estimation technique is proposed, where rated load conditions are considered at the first stage in order to reduce the number of parameters to be identified. The UKF technique requires three measurements from the power transformer (load factor, oil temperature, and hot-spot temperature), along with the ambient temperature, all of which are easily available during factory tests.

A case study has been simulated, where the maximum relative estimation error remains under 3%. It has also shown that the estimation errors are not significantly affected by the number of intermediate load factors adopted at the second stage of the estimation process. As expected, increasing levels of measurement errors tend to deteriorate the performance of the UKF estimator, but even for unrealistically high error values (10%), the maximum estimation error is acceptable in relative terms (7.5%).

In terms of convergence and accuracy, the proposed technique performs significantly better than the EKF, which suffers from the non-linearity of the model when all parameters become unknown.

Finally, the impact of the parameter estimation errors on the accuracy of the hot-spot temperature evolution, during the transformer field operation, has been assessed through a simulation spanning a week, using as inputs only the load factor and the ambient temperature. The results obtained show that the hot-spot temperature obtained with the estimated model is sufficiently close to that of the exact model, with a maximum absolute error lower than 4 °C for reduced values of the load factor, and approximately 2 °C as the rated transformer load is approached.

The proposed technique can fill the existing gap in real-time thermal modeling of power transformers, by allowing manufacturers to perform straightforward in-house tests, where the load conditions can be controlled, which in turn will let their customers easily monitor the hot-spot temperature during the field operation, based only on the actual load and ambient temperature.

Appendix A

The implementation of the EKF formulation also involves two stages of estimation, as those presented for the UKF. For the first stage, the discrete form of the model dynamic equations is as follows:

$$\theta_{o,k}=\theta_{o,k-1}+\frac{\Delta t}{T_{o,k-1}}(\Delta\theta_{or,k-1}-\theta_{o,k-1}+\theta_{a,k-1}) \tag{A1}$$

$$\Delta\theta_{h1,k}=\Delta\theta_{h1,k-1}+\frac{\Delta t}{T_{1,k-1}}(C_{1,k-1}-\Delta\theta_{h1,k-1}) \tag{A2}$$

$$\Delta\theta_{h2,k}=\Delta\theta_{h2,k-1}+\frac{\Delta t}{T_{2,k-1}}(C_{2,k-1}-\Delta\theta_{h2,k-1}) \tag{A3}$$

$$T_{1,k}=T_{1,k-1} \tag{A4}$$

$$T_{2,k}=T_{2,k-1} \tag{A5}$$

$$C_{1,k}=C_{1,k-1} \tag{A6}$$

$$C_{2,k}=C_{2,k-1} \tag{A7}$$

$$T_{o,k}=T_{o,k-1} \tag{A8}$$

$$\Delta\theta_{or,k}=\Delta\theta_{or,k-1} \tag{A9}$$

The EKF uses the Jacobian matrix of the state function at time k, namely $\boldsymbol{F}_k$, where each element of this matrix is defined as:

$$F_k^{i,j}=\frac{\partial x_{i,k}}{\partial x_{j,k-1}} \tag{A10}$$

Using the above definition, the partial derivatives of (A1)-(A9) must be calculated, yielding the following expressions for the non-null terms, where the correspondences with the elements of $\boldsymbol{F}_k$ are indicated:

$$F_k^{1,1}=1-\frac{\Delta t}{T_{o,k-1}} \tag{A11}$$

$$F_k^{1,8}=-\frac{\Delta t(\Delta\theta_{or,k-1}-\theta_{o,k-1}+\theta_{a,k-1})}{T_{o,k-1}^2} \tag{A12}$$

$$F_k^{1,9}=\frac{\Delta t}{T_{o,k-1}} \tag{A13}$$

$$F_k^{2,2}=1-\frac{\Delta t}{T_{1,k-1}} \tag{A14}$$

$$F_k^{2,4}=-\frac{\Delta t(C_{1,k-1}-\Delta\theta_{h1,k-1})}{T_{1,k-1}^2} \tag{A15}$$

$$F_k^{2,6}=\frac{\Delta t}{T_{1,k-1}} \tag{A16}$$

$$F_k^{3,3}=1-\frac{\Delta t}{T_{2,k-1}} \tag{A17}$$

$$F_k^{3,5}=-\frac{\Delta t(C_{2,k-1}-\Delta\theta_{h2,k-1})}{T_{2,k-1}^2} \tag{A18}$$

$$F_k^{3,7}=\frac{\Delta t}{T_{2,k-1}} \tag{A19}$$

$$F_k^{i,i}=1 \quad i=4,5,...,9 \tag{A20}$$

Note that the measurement equation (23) is linear, so that its Jacobian matrix is trivial. Once these Jacobian matrices are obtained, the iterative algorithm of the EKF is implemented, as described in [25]. Similar derivations (not reported here) are made for the second stage of the estimation

technique proposed in this paper, with a reduced number of parameters included in the augmented state vector.

REFERENCES

[1] M. A. Tsili, E. I. Amoiralis, A. G. Kladas *et al*., "Hybrid numerical-analytical technique for power transformer thermal modeling," *IEEE Transactions on Magnetics*, vol. 45, no. 3, pp. 1408-1411, Mar. 2009.

[2] M. Akbari and A. Rezaei-Zare, "Transformer bushing thermal model for calculation of hot-spot temperature considering oil flow dynamics," *IEEE Transactions on Power Delivery*, vol. 36, no. 3, pp. 1726-1734, Jun. 2021.

[3] P. Penabad-Duran, X. M. Lopez-Fernandez, and J. Turowski, "3D nonlinear magneto-thermal behavior on transformer covers," *Electric Power Systems Research*, vol. 121, pp. 333-340, Apr. 2015.

[4] S. Taheri, A. Gholami, I. Fofana *et al*., "Modeling and simulation of transformer loading capability and hot spot temperature under harmonic conditions," *Electric Power Systems Research*, vol. 86, pp. 68-75, Mar. 2012.

[5] O. Amoda, D. Tylavsky, W. Knuth *et al*., "Sensitivity of estimated parameters in transformer thermal modeling," in *Proceedings of 41st North American Power Symposium*, Starkville, USA, Nov. 2019, pp. 1-6..

[6] V. Galdi, L. Ippolito, A. Piccolo *et al*., "Parameter identification of power transformers thermal model via genetic algorithms," *Electric Power Systems Research*, vol. 60, no. 2, pp. 107-113, Dec. 2001.

[7] *Power Transformers – Part 7: Loading Guide for Mineral-oil-immersed Power Transformers*, IEC 60076-7-2018, 2018.

[8] S. Song, H. Wei, Y. Lin *et al*., "A holistic state estimation framework for active distribution network with battery energy storage system," *Journal of Modern Power Systems and Clean Energy*, vol. 10, no. 3, pp. 627-636, May 2022.

[9] T. Zhang, W. Zhang, Q. Zhao *et al*., "Distributed real-time state estimation for combined heat and power systems," *Journal of Modern Power Systems and Clean Energy*, vol. 9, no. 2, pp. 316-327, Mar. 2021.

[10] J. Zhao, A. Gómez-Expósito, M. Netto *et al*., "Power system dynamic state estimation: motivations, definitions, methodologies, and future work," *IEEE Transactions on Power Systems*, vol. 34, no. 4, pp. 3188-3198, Jul. 2019.

[11] J. Zhao, M. Netto, Z. Huang *et al*., "Roles of dynamic state estimation in power system modeling, monitoring and operation," *IEEE Transactions on Power Systems*, vol. 36, no. 3, pp. 2462-2472, May 2021.

[12] A. Onat, "A novel and computationally efficient joint unscented Kalman filtering scheme for parameter estimation of a class of nonlinear systems," *IEEE Access*, vol. 7, pp. 31634-31655, Mar. 2019.

[13] A. Yu, Y. Liu, J. Zhu *et al*., "An improved dual unscented Kalman filter for state and parameter estimation," *Asian Journal of Control*, vol. 18, pp. 1427-1440, 2016, Oct. 2015.

[14] N. Živković and A. T. Sarić, "Detection of false data injection attacks using unscented Kalman filter," *Journal of Modern Power Systems and Clean Energy*, vol. 6, no. 5, pp. 847-859, Sept. 2018.

[15] J. Feng, F. Cai, J. Yang *et al*., "An adaptive state of charge estimation method of lithium-ion battery based on residual constraint fading factor unscented Kalman filter," *IEEE Access*, vol. 10, pp. 44549-44563, Apr. 2022.

[16] H. Li, K. Pei, and W. Sun, "Dynamic state estimation for power system based on the measurement data reconstructed by RGAN," *IEEE Access*, vol. 9, pp. 92578-92585, Jun. 2021.

[17] M. A. González-Cagigal, J. A. Rosendo-Macías, and A. Gómez-Expósito, "Parameter estimation of fully regulated synchronous generators using unscented Kalman filters," *Electric Power Systems Research*, vol. 168. pp. 210-217, Mar. 2019.

[18] F. Q. López-Manzanares, "Aplicación de filtro de Kalman a la estimación de parámetros térmicos en transformadores de aceite." B.S. thesis, University of Seville, Seville, Spain, 2021.

[19] D. Simon, *Optimal State Estimation: Kalman, H Infinity and Nonlinear Approaches*. New York: John Wiley & Sons, 2006.

[20] E. A. Wan and R. van der Merwe, "The unscented Kalman filter for nonlinear estimation," in *Proceeding of Adaptive Systems for Signal Processing, Communications, and Control Symposium*, Lake Louise, Canada, Oct. 2000, pp. 153-158.

[21] R. Barlik, M. Nowak, P. Grzejszczak *et al*., "Estimation of power losses in a high-frequency planar transformer using a thermal camera," *Archives of Electrical Engineering*, vol. 65, pp. 613-627, Sept. 2016.

[22] S. Julier, "The scaled unscented transformation," in *Proceedings of the 2002 American Control Conference*, Anchorage, USA, May 2002, pp. 4555-4559.

[23] Open Data. (2022, Mar.). Index of /climate_environment/. [Online]. Available: https://opendata.dwd.de/climate_environment/

[24] J. J. Hyun and L. Hyung-Chul, "Analysis of scaling parameters of the batch unscented transformation for precision orbit determination using satellite laser ranging data," *Journal of Astronomy and Space Sciences*, vol. 28, pp. 183-192, Sept. 2011.

[25] H. W. Sorenson and A. R. Stubberud, "Non-linear filtering by approximation of the a posteriori density," *International Journal of Control*, vol. 8, pp. 33-51, Jul. 1968.

Miguel Ángel González-Cagigal received the Industrial Engineer, M. S., and Ph. D. degrees from the University of Seville, Seville, Spain, in 2017, 2019, and 2021, respectively. He is currently with the Department of Electrical Engineering, University of Seville. His research interests include dynamic state estimation and operation of electric power systems.

José Antonio Rosendo-Macías received the Electrical Engineering and Ph.D. degrees from the University of Seville, Seville, Spain. Since 1992, he has been with the Department of Electrical Engineering, University of Seville, where he is currently a Professor. His primary research interests are dynamic state estimation, digital signal processing, digital relaying, and distribution reliability.

Antonio Gómez-Expósito received the Ph.D. degree in electrical engineering from the University of Seville, Seville, Spain, in 1985. He is currently the Endesa Red Industrial Chair Professor with the University of Seville. His primary research interests include optimal power system operation, state estimation, digital signal processing, and control of flexible AC transmission system devices.